Transactions on Engineering Sciences vol 4, © 1994 WIT Press, www.witpress.com, ISSN 1743-3533

Micromechanics analysis of hybrid woven fabric composites under tensile and compression load

U. Leischner, A.F. Johnson

German Aerospace Establishment (DLR), Institute for Structures and Design, D-70569 Stuttgart, Germany

ABSTRACT

An FE model for a carbon/aramid hybrid composite with a 2/2 twill woven fabric is described. Stiffness and strength properties are computed and compared with the results of simpler micromechanics models for woven fabric composites and with test data. The FE model is used to study the progressive failure process in hybrid composites under both tensile and compressive loads.

INTRODUCTION

In hybrid fabric composite laminates fibres with high strength and stiffness but modest failure strain, such as carbon fibres, may be combined with relatively ductile aramid or polyethylene fibres. Hybrids offer therefore advantages regarding structural integrity and sustained load under crash or impact conditions. However, hybrid fabrics contain a large number of microstructural parameters (type and proportion of each fibre, weave pattern, fibre volume fraction, etc.), which strongly influence the composite properties. Thus in order to realise the advantages of hybridisation, methods are needed for understanding and tailoring hybrid composite properties. Several micromechanical models for woven fabric (WF) composites have been developed [1]-[6] and incorporated into PC programs [7],[8], which may be used to calculate elastic and strength properties of hybrid WF composites. In these theories the local elastic properties are averaged over the lamina thickness, thus only average stresses are obtained which reduces the accuracy of strength calculations. Little is known about the strength properties of WF composites in compression, which are important in composites crash structures.

After assessing the validity of the micromechanics models a finite element analysis (FEA) of a carbon/aramid hybrid composite with 2/2 twill WF is described which is based on a 3-D FEA model of the fabric weave in a repeating

cell in the composite. Nonlinear large strain analyses for tension and compression are used to model the changes in properties due to fibre reorientations. The computed stress distributions in the rovings enable microstructural damage modes to be identified and the influence of hybridisation on these failure mechanisms to be studied. Results are compared with test data on the stiffness and strength properties of carbon/aramid hybrid WF composites.

MICROMECHANICS MODELLING OF WF COMPOSITES

Micromechanics models

Several micromechanics models have been developed for predicting the properties of WF composites. One of the first was the mosaic model [1] in which the fabric is replaced by a mosaic of cross-ply elements. Since fibre crimp is neglected, which has a strong influence on WF properties in plain weave fabrics, the mosaic model gives only approximate bounds on properties. An improvement is the crimp model [1] which includes both fibre continuity and fibre undulations. For the fabric models we adopt a global (x,y,z) coordinate system (Fig. 1) in which x and y are in the fill and warp directions, with z through the fabric thickness. In the crimp model the coefficients of the stiffness matrix [A] of the unit cell in Fig. 1 are determined by classical laminate theory (CLT), which are then integrated along the crimped roving to take into account the change in stiffness due to the angle between the rovings and the x-axis. The crimp model is extended to hybrids in [2] and a similar model, also valid for hybrids, with a different crimp shape function is given in [3].

The crimp models are essentially 2-D since the properties are integrated through the x-z plane, but they take no account of the changing shape of the rovings in the transverse y-direction. These effects are included in the soft mosaic theory (SMT) of [4],[5] and the element array model of [6]. In these theories the cell elements are sliced up in the x and y directions, CLT is used for the slice properties and the element properties are determined by integration over x and y. In SMT up to 36 types of cell element are identified for a hybrid fabric, which are then fitted together to match the fabric pattern. Thus SMT combines features of the mosaic model with more accurate unit cell properties. In order to calculate strength properties in SMT, the CLT is used to calculate failure stresses in each mosaic element using a Tsai-Wu failure criterion. Since this is usually a transverse failure in the rovings the predicted strengths are "first ply failure" (fpf) damage stress. In [3] the failure of the crimped roving under axial and shear stresses arising from the axial load are analysed. By neglecting transverse stresses in the roving the model is able to estimate the ultimate strength of a WF composite at failure of the axially loaded rovings.

Predicted WF composite properties

Computer programs are required to use the models for the prediction of WF properties. Commercially available programs are WFM [7] for the mosaic, crimp and bridging models, and MIKROLAM [8] which contains the crimp

model [3] along with models for UD and mat composites. SMT was developed at the DLR and exists as a Fortran program. Detailed in-house test results are also available for the mechanical properties of WF/epoxy composites [9] with 2/2 twill 245g/m² carbon fabric and 2/2 twill 200g/m² carbon/aramid hybrid fabric reinforcements. These test results were used to compare the validity of the micromechanics models and the FE model of the next section.

Table 1 Materials data used in the micromechanics and FE models

	Carbon Roving	Aramid Roving	Carbon Fibre	Aramid Fibre	Matrix
	$v_{fr} = 0.59$	$v_{fr} = 0.48$	T300	Kevlar 49	Bakelite L20/SL
E_1 [GPa]	137.00	65.50	230.00	133.00	3.20
E_2 [GPa]	9.57	5.13	24.00	7.00	3.20
G_{12} [GPa]	4.74	3.16	50.00	12.00	1.19
G_{23} [GPa]	3.23	2.08	33.00	8.00	1.19
ν_{12} [-]	0.309	0.364	0.28	0.38	0.35
ν_{23} [-]	0.45	0.45	0.35	0.40	0.35
σ_{1t} [MPa]	1760	1133	3240	3620	77
σ_{1c} [MPa]	1760	221	3240	460	85
σ_{2t} [MPa]	50	29	60	33	77
σ_{2c} [MPa]	210	74	248	84	85
τ_{12} [MPa]	84	30	100	37	35

The materials data used for the calculations are shown in Table 1, referred to the local (1,2,3) axes in the rovings, where 1 is the roving axial direction, 2 is transverse in the y-direction and 3 through the roving thickness. The FE model and WFM require the properties of the matrix and the UD fibre rovings, whilst SMT and MIKROLAM use fibre and matrix data to calculate rovings properties. The UD rovings have a local fibre volume fraction v_{fr} , which depends on the fibre wet-out properties. The global v_f in the WF composite is less than v_{fr} and is varied in the models by changing the thickness of the resin layers between the fabric plies. Measurements were made on a cross-section cut from the WF laminates to determine roving geometry and spacing. Fig.1 shows the notation used for the fabric cell geometry and the measured data for the carbon and hybrid fabrics are listed in Table 2.

Table 2 Fabric geometry in mm

	a_{ef}	a_{ew}	a_{tf}	a_{tw}	h_t	h	u_f	u_w
2/2 carbon	1.7	1.7	1.3	1.3	0.35	0.35	0.6	0.6
2/2 hybrid	1.8	1.8	1.5	1.5	0.30	0.35	0.6	0.6

Table 3 compares the moduli and strengths calculated for the 2/2 twill carbon and hybrid fabrics using the three micromechanics programs with test data. Note that WFM is not valid for hybrids, does not include strength properties and has 6 different stiffness models. The WFM crimp model with warping constraint was chosen as most relevant to the fabrics here. The table shows reasonably good agreement between measured and predicted E-moduli and Poisson's ratios. The predicted shear moduli are much higher than the measured values, which were however obtained from 45° tensile tests and are considered to be low. The measured strengths are ultimate strengths σ_{xt}, σ_{xc} in tension and

Table 3 Comparison of measured and calculated WF properties (# fpf damage stress, * lpf ultimate strength)

	SMT	WFM	Mikrolam	FE	Experiment
	2/2 twill carbon WF, 245g/m^2, v_f = 0.40				
E_x [GPa]	50.15	45.60	50.38	48.94	49.38
G_{xy} [GPa]	-	4.10	3.58		2.36
ν_{xy} [-]	0.0974	0.0604	0.050	0.041	0.059
σ_{xt} [MPa]	57$^{\#}$	-	435*	241$^{\#}$/579*	599*
σ_{xc} [MPa]	119$^{\#}$	-	460*	254$^{\#}$/560*	593*
τ_{xy} [MPa]	-	-	83*		98*
	2/2 twill carbon/aramid hybrid WF, 200g/m^2, v_f = 0.36				
E_x [GPa]	36.42	-	33.66	36.61	35.86
G_{xy} [GPa]	-	-	2.70		1.41
ν_{xy} [-]	0.0941	-	0.060	0.0475	0.073
σ_{xt} [MPa]	44$^{\#}$	-	298*	153$^{\#}$/430*	413*
σ_{xc} [MPa]	63$^{\#}$	-	111*	109$^{\#}$/413*	291*
τ_{xy} [MPa]	-	-	34*		77*

compression and the shear strength τ_{xy}. The SMT strengths are between 10 - 20% of the measured strengths, however as stated above these are interpreted as fpf damage stresses. The MIKROLAM strength predictions are much higher, but still about 25% below the measured values. We conclude that the micromechanics models all give a good prediction of WF stiffness properties, but for a better understanding of damage and failure behaviour more detailed numerical modelling is required.

FE MODELLING OF WF COMPOSITES

FE Model

The FE analysis is based on the detailed geometry model of a unit cell in a hybrid WF composite loaded in tension and compression in the fibre (warp or fill) directions. The analysis was carried out with the ANSYS 5.0 [10] FE software on an HP 735 workstation. The E-moduli, Poisson's ratios, tensile and compression strengths are determined for a carbon and carbon/aramid hybrid WF for comparison with the micromechanics models and the test results. Failure processes are studied in some detail including the influence of nonlinear geometrical effects such as fibre straightening and crimping.

Fig. 2 shows the unit cell with the FE mesh in the model of a 2/2 twill hybrid WF composite. The cell is 7.2 mm square, 0.35 mm thick, and represents a single internal WF ply in a multiply laminate. Details of the weave geometry are as in Table 2, with the cell side length a = $4a_{cw}$, equivalent to 4 mosaic elements (Fig. 1). No distinction is made between warp and fill directions in the model. In comparison with the model of a plain weave single fibre fabric used in [11], a 2/2 hybrid fabric requires the large repeating cell shown which has no symmetry to exploit in the analysis. Ansys SOLID45 8-node volume elements were used, with each roving cross section being modelled by 12 elements. The complete

model contained 8400 elements with 9200 nodes and requires considerable computational effort and storage requirements for a nonlinear analysis.

The load and boundary conditions on the unit cell are as follows. A uniform strain ε_x is applied in the x-direction through applied nodal displacements:

$$u_x = 0 \text{ on } x = 0, \qquad u_x = a\varepsilon_x \text{ on } x = a,$$

with free lateral contraction/expansion allowed in the y- and z-directions. Symmetry and continuity conditions are also applied to the unit cell. Thus it is assumed that opposite faces of the cell remain plane, with corresponding positions having equal in-plane displacements, eg

$$u_y(0,y,z) = u_y(a,y,z), \qquad u_z(0,y,z) = u_z(a,y,z) \qquad \text{for each } (y,z),$$

which are applied pointwise as coupled degrees of freedom. These boundary conditions were chosen after trial analyses with the more precise conditions discussed in [11], in which the plane face assumption was relaxed. Thus the out-of-plane displacements of corresponding nodes on opposite faces were coupled to ensure continuity between cells. This increased the computation time of the FE analysis through a higher wavefront, but led to negligible differences in computed results. Thus it was concluded that the unit cell here is big enough to be a representative element of WF composite and the plane face assumption with reduced wavefront could be used.

The carbon and aramid rovings are modelled as transverse isotropic elastic materials and for the volume elements a full set of 5 elastic constants are required, with the matrix material assumed to be isotropic elastic. The materials data used in the analysis are listed in Table 1. A geometrically nonlinear analysis was carried out in which the maximum applied strain $\varepsilon_x = 0.02$ is applied in steps. At each step the strain is applied incrementally and equilibrium iterations are used with adjusted stiffness matrices to obtain a convergent solution at each substep. For each strain step the total resultant nodal forces F_x on the face x = a were summed to give the effective true stress σ_x and hence the nonlinear stress-strain curves in Fig. 3 were determined. Values of the initial tensile modulus $E_x = \sigma_x/\varepsilon_x$ and Poisson's ratio $\nu_{xy} = -\varepsilon_y/\varepsilon_x$ were then calculated. Information on failure processes follows from a study of element stresses in the local element (1,2,3) coordinate systems and by the application of maximum stress failure criteria in the rovings and matrix.

FE results

The computed values of E_x and ν_{xy} for the 2/2 twill carbon and carbon/aramid hybrid WF composites are listed in Table 3. Moduli show excellent agreement to within 2% of the test data, however Poisson's ratios are much lower and are not better than the micromechanics predictions. The computed stress-strain curves in tension and compression in Fig. 3 are marked with the microstructural failure points obtained from study of the matrix and roving element stresses. These WF composite failure stresses σ_x are listed in more detail in Table 4. In the table the index n = 1,2,3 shows which element stress σ_1, σ_2, σ_3 has failed,

and t,c indicate tensile or compressive failure. We note that the maximum stresses usually occur at the crimp in the loaded fibres where local bending stresses are superimposed on a fairly uniform axial tensile or compression stress. For example, Table 4 shows that the first damage in the hybrid fabric under compression is at σ_x = 109 MPa when the aramid x-rovings fail in compression. This is followed by transverse tensile failure in the aramid y-rovings through their thickness (3-direction) at 150 MPa, matrix failure at 171 MPa and ultimate failure at 413 MPa when the carbon x-rovings fail. Thus study of Fig. 3 and Table 4 give important information about damage mechanisms in carbon and hybrid composites. We see that in the hybrid under tension the initial damage is transverse tensile failure of the loaded carbon x-rovings, whilst under compression it is a compression failure in the loaded aramid x-rovings.

Table 4 WF stresses σ_x at which microdamage occurs
(fpf = 1st damage, lpf = failure of carbon x-rovings, ⊕ = no damage)

	n	carbon x-roving	carbon y-roving	aramid x-roving	aramid y-roving	matrix
hybrid wf compression	1	lpf **413** c	⊕	fpf **109** c	⊕	171 c
	2	⊕	⊕	⊕	⊕	
	3	⊕	189 t	⊕	150 t	
hybrid wf tension	1	lpf **430** t	⊕	⊕	⊕	170 t
	2	249 t	162 t	234 t	177 t	
	3	fpf **153** t	⊕	⊕	⊕	
carbon wf compression	1	lpf **560** c	⊕			fpf **254** c
	2	⊕	⊕			
	3	⊕	260 t			
carbon wf tension	1	lpf **579** t	⊕			250 t
	2	⊕	⊕			
	3	fpf **241** t	⊕			

The computed initial damage stresses (fpf) and ultimate strengths (lpf) are also listed in Table 3. Comparison with the micromechanics predictions shows the fpf stresses to be much higher than those from SMT, whilst the lpf stresses are above the MIKROLAM values and except for the hybrid compression case are within 6% of the measured strength data, which is a satisfactory agreement. The stress-strain curves in Fig. 3 are close to linearity indicating that the expected influence of fibre straightening in tension and crimping in compression included in the nonlinear analysis are not very significant in 2/2 twill fabrics. These effects are expected to be more important in plain weave fabrics. The results shown take no account of the change in the WF composite properties due to the initial damage in the rovings and matrix. This is currently under investigation using nonlinear materials properties to replace the linear elastic behaviour. A failure mode identified here, which is important in impact applications with hybrids, is of aramid fibres loaded in compression which exhibit elastic-plastic behaviour [12]. Thus the aramid roving compression strength value in Table 1 is in fact a yield stress. This effect was simulated in a further FE analysis using an orthotropic elastic-plastic material model for the aramid rovings. Preliminary results are included in Fig. 3 for the compression

load case. Because of the complexity of the model there were some convergence problems at higher strains and the dotted extension to the curve were obtained by extrapolation to ultimate failure. Nonetheless these initial results are encouraging since they indicate that compressive yielding in the aramid fibres leads to a nonlinear stress-strain response in the hybrid composite under compression with stress softening or plastification. The estimated ultimate compression strength of 350 MPa is then lower than the elastic value and much nearer to the measured strength.

CONCLUSIONS

1. The WF models investigated all gave satisfactory predictions of stiffness properties and are valuable tools for studying WF composites, including hybrids, with different weave patterns. The FE model was more accurate, but inflexible, and is less suited to the routine determination of WF stiffnesses.
2. The micromechanics strength models, when available, gave uncertain predictions of WF strength properties and required insight from the user to distinguish between damage and failure. However, the strength model in MIKROLAM [3],[8] gave a reasonable estimate of WF strengths.
3. The FE model developed here gave valuable information about damage modes in hybrid WF composites with good estimates of ultimate strength properties. Improvements are needed with nonlinear materials models to simulate damage progression before ultimate failure in WF composites .

Acknowledgement: The authors wish to thank their colleagues Ch. Kindervater and K. Stellbrink for valuable discussions.

REFERENCES

1. Ishikawa, T. and Chou, T.-W. 'One Dimensional Micromechanical Analysis of WF Composites' *AIAA Journal*, Vol.21, pp.1714-1721,1983.
2. Ishikawa, T. and Chou, T.-W. 'Stiffness and Strength Behaviour of WF Composites' *J Mat. Sci.*, Vol.17, pp. 3211-3220, 1982.
3. Stellbrink, K. 'Abschätzung mechanischer Eigenschaften gewebeverstärkter Faserkunststoffverbunde' *DLR Report*, IB 435-92/16, 1992.
4. Mai, H.U. 'A Soft Mosaic Theory for Elastic and Strength Properties of Hybrid Woven Composites' *DLR Report*, IB 435-85/20, 1985.
5. Mai, H.U. and Hienstorfer, W.G. 'Die Soft-Mosaik-Theorie: Eine Methode zur Bestimmung der elastischen Kenngrössen und des Festigkeitsverhaltens von Gewebe-laminaten' *DGLR-Jahrestagung, Jahrbuch I*, Darmstadt, 1988.
6. Naik, N.K. *Woven Fabric Composites* Technomic, Lancaster PA, 1994.
7. *Woven fabric Micromechanics WFM* Technomic, Lancaster PA, 1991.
8. *MIKROLAM* Stellbrink, K, Drosselweg 7, D-71126 Gäufelden, 1993.
9. Glaser, J 'Untersuchung der elastischen Kenngrößen u. des Festigkeitsverhaltens vonFaserkunststoffverbunden mit Gewebeverstärkung' *DLR Report*, IB 435-87/24, 1987.
10. *ANSYS 5.0* Swanson Analysis Systems Inc, PO Box 6, Houston, PA.
11. Bhandarker, R.K., Agarwal, A. and Dasgupta, A. 'Micromechanical Simulation of Thermomechanical and Thermal Properties of WF Composites' in CADCOMP 92 (Ed. Advani, S.G. et al), pp. 547-558, *CAD in Composite Material Technology III* CMP, Southampton, 1992.
12. *Data Manual for Kevlar 49 Aramid* Dupont de Nemours Int. S.A ,Geneva.

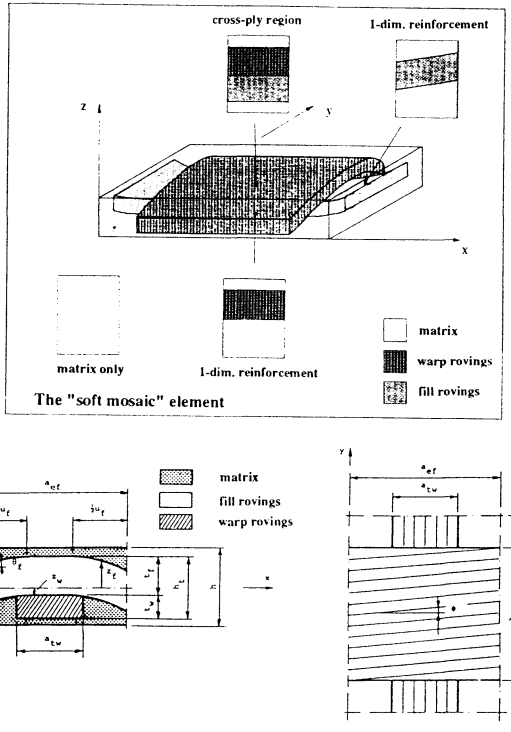

Fig. 1 Geometry of the fabric element in a micromechanics model.

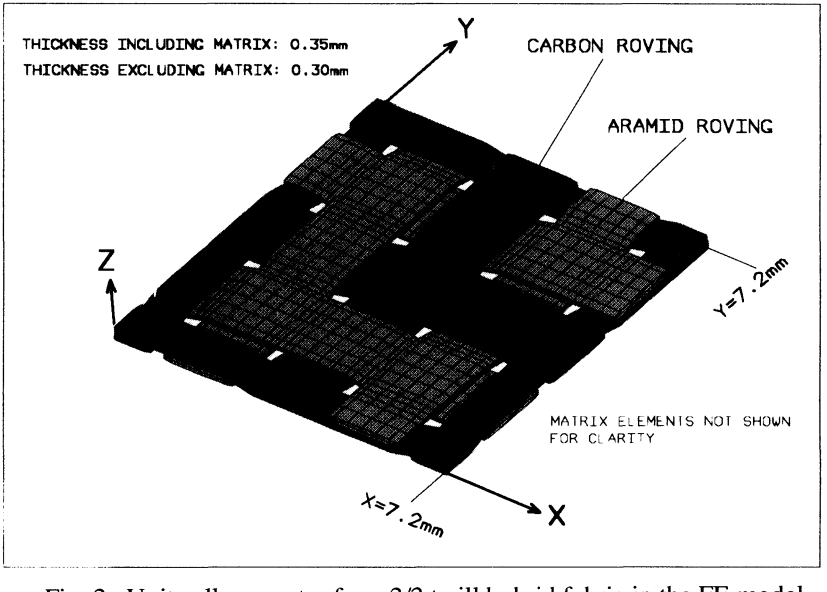

Fig. 2 Unit cell geometry for a 2/2 twill hybrid fabric in the FE model.

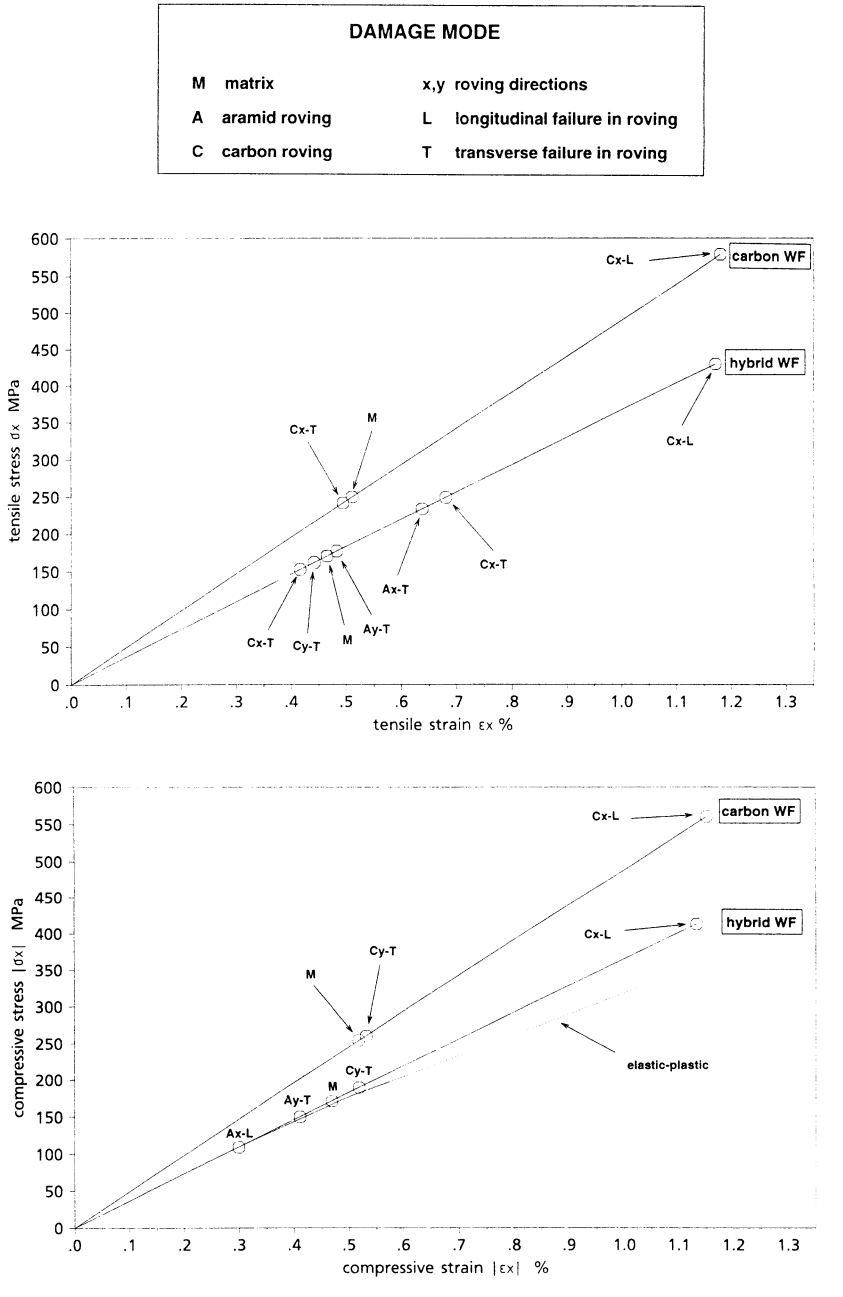

Fig. 3 Stress-strain curves in tension and compression for 2/2 twill carbon and carbon/aramid hybrid WF composites showing damage modes.